Double-layer indium doped zinc oxide for silicon thin-film solar cell prepared by ultrasonic spray pyrolysis*

Jiao Bao-Chen(焦宝臣), Zhang Xiao-Dan(张晓丹)†, Wei Chang-Chun(魏长春), Sun Jian(孙 建), Ni Jian(倪 牮), and Zhao Ying(赵 颖)

Institute of Photo-electronic Thin Film Devices and Technology, Nankai University, Tianjin 300071, China

(Received 20 July 2010; revised manuscript received 29 November 2010)

Indium doped zinc oxide (ZnO:In) thin films were prepared by ultrasonic spray pyrolysis on corning eagle 2000 glass substrate. 1 and 2 at.% indium doped single-layer ZnO:In thin films with different amounts of acetic acid added in the initial solution were fabricated. The 1 at.% indium doped single-layers have triangle grains. The 2 at.% indium doped single-layer with 0.18 acetic acid adding has the resistivity of 6.82×10^{-3} $\Omega\cdot$cm and particle grains. The double-layers structure is designed to fabricate the ZnO:In thin film with low resistivity (2.58×10^{-3} $\Omega\cdot$cm) and good surface morphology. It is found that the surface morphology of the double-layer ZnO:In film strongly depends on the substrate-layer, and the second-layer plays a large part in the resistivity of the double-layer ZnO:In thin film. Both total and direct transmittances of the double-layer ZnO:In film are above 80% in the visible light region. Single junction a-Si:H solar cell based on the double-layer ZnO:In as front electrode is also investigated.

Keywords: indium doped zinc oxide thin film, ultrasonic spray pyrolysis, double-layer structure, solar cell

PACS: 73.61.Ga, 81.15Rs, 88.40.jj **DOI:** 10.1088/1674-1056/20/3/037306

1. Introduction

Zinc oxide (ZnO) is an n-type semiconductor with a band gap of 3.37 eV, and has a hexagonal wurtzite structure.[1] Due to its high optical transparency in the visible light region, high electrical conductivity, easy preparation, and high stability in hydrogen plasma, ZnO film as transparent conductive oxide (TCO) has been widely used in solar cells.[2−4] ZnO-TCO with light trapping structure is very important for silicon-based thin film solar cells. Metal organic chemical vapour deposition (MOCVD)[5−8] and sputtering combined with chemical etching[9,10] are commonly used to fabricate ZnO-TCO with light trapping structure, but the cost is high. Consequently, there is an urgent necessity for a low-cost method to prepare ZnO-TCO.

Ultrasonic spray pyrolysis (USP) has received extra attention because of its simplicity, suitability for product industrialization, and cost-effectiveness. Utilizing USP to prepare ZnO-TCO is very potential. Doping with indium can improve the electrical properties and change the surface morphology of the sprayed ZnO thin films, which has been studied by several groups.[11−13] However, the good electrical properties and light trapping structures can not be achieved easily at the same time. Only Wienker *et al.* have done some research.[14,15] Hence, further studying of the spray-deposited ZnO thin films with good electrical properties and light trapping structure is meaningful.

In this work, the sprayed-deposited single-layer ZnO:In thin films with different amounts of acetic acid added in the initial solution were investigated. In order to obtain ZnO:In thin films with good electrical properties and light trapping structure, ZnO:In thin films with double-layer structure were deposited by USP. Finally, the performance of single junction a-Si:H solar cell fabricated on both the double-layer ZnO:In and the ASAHI U-type SnO_2:F as front electrode were compared.

*Project supported by Hi-Tech Research and Development Program of China (Grant Nos. 2007AA05Z436 and 2009AA050602), Science and Technology Support Project of Tianjin (Grant No. 08ZCKFGX03500), the National Basic Research Program of China (Grant Nos. 2011CB201605 and 2011CB201606), the National Natural Science Foundation of China (Grant No. 60976051), International Cooperation Project between China-Greece Government (Grant No. 2009DFA62580), and Program for New Century Excellent Talents in University of China (Grant No. NCET-08-0295).

†Corresponding author. E-mail: xdzhang@nankai.edu.cn

© 2011 Chinese Physical Society and IOP Publishing Ltd

2. Experimental

The films were deposited by USP on corning eagle 2000 glass substrates. The initial solution was 0.2 mol/L zinc acetate diluted in ethanol and water (3:1 volume ratio). Indium acetate was added in the initial solution for indium doping. The In/Zn ratios were 1 and 2 at.%. For the 1 at.% indium doped ZnO films, the different amounts of acetic acid were added in the initial solution in volume proportion of 0.04, 0.08, 0.1, 0.12 (acetic acid/the initial solution); For the 2 at.% indium doping, the different amounts of acetic acid were added at 0.16, 0.18, 0.20, 0.22, 0.24.

After the corning eagle 2000 substrate was heated to 750 K, the aerosol of the initial solution was nebulized by an ultrasonic agitation with 1.7 MHz, and transported into the growth chamber by air at a flow rate of 11 L/min.

Single junction a-Si:H thin-film solar cells were deposited on both the spray-deposited double-layer ZnO:In and the Asahi U-type SnO_2:F. The a-Si:H based layers were deposited by RF-PECVD. The solar cells have the following structure: glass/TCO/p-type a-SiC:H layer (30 nm)/intrinsic a-Si:H absorber layer (300 nm)/n-type μ-Si:H layer (30 nm)/Al. The back contact is 400-nm-thick aluminum. The cell area of 0.253 cm^2 was defined by evapourating the metal back contacts through a mechanical mask.

X-ray diffraction (XRD, X'Derpro Co. λ_{Cu} = 1.542 Å, 1 Å = 0.1 nm) analysis was performed to investigate the crystallographic structure of the ZnO:In thin films. The surface morphology was observed by field emission scanning electron microscope (FE-SEM, JSM-6700F). The thin film thicknesses were measured using a step profiler (AMBIOS-XP2). The electrical properties were investigated by Hall measurements (Accent HL5500 PC) with the Van der Pauw method. The optical transmittance of thin films was evaluated by UV–visible–NIR spectrometer (Cary 5000 UV–VIS produced by Varian Company). The root-mean square roughness (δ_{rms}) of thin films was taken on an area of 10×10 μm^2 in a contact mode with an atomic force microscope (AFM) (SPA-400 SPM UNIT product by Seiko Instruments Inc.). The current–voltage (J–V) characteristics of solar cells were measured using a 1000 W/m^2 AM 1.5 steady-state solar simulator.

3. Results and discussions

3.1. Single-layer ZnO:In thin film property

The resistivity of the single-layer ZnO:In thin films with different amounts of acetic acid are shown in Fig. 1. When the films were 1 at.% indium doped, the resistivity decreased with increasing the acetic acid. For the added acetic acid more than or equal to 0.1, the resistivity increased slightly. The lower resistivity (7.14×10^{-3} $\Omega\cdot$cm) was achieved at 0.1 acetic acid. For the 2 at.% indium doped films, the resistivity changing trend was the same as the 1 at.% indium doped films. However, it did not change greatly. The lower resistivity was obtained at 0.18 acetic acid added. Among all the single layers, the lowest resistivity (6.82×10^{-3} $\Omega\cdot$cm) was obtained at the 2 at.% indium doped and 0.18 acetic acid added. The thickness for all the single-layers is about 300 nm.

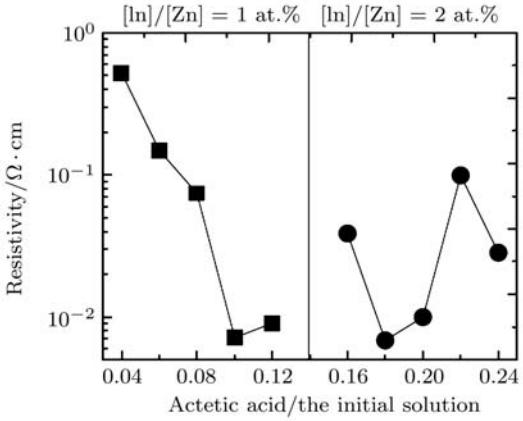


Fig. 1. Resistivity of the single-layer ZnO:In thin films with different amounts of acetic acid added.

Some papers have reported that the acetic acid was commonly utilized to avoid the precipitation of Zn-OH species[16] and change the pH of initial solution.[17] Moreover, the acetic acid can supply [AC^-] due to the ionization of the acetic acid. The complexes can be formed by [AC^-] and the metal ions ([Zn^{2+}], [In^{3+}]). Their coordination numbers are 1 and 4, respectively.[18] The state of indium is similar to zinc owe to the complexes, which is favourable for the indium doping. Moreover, when the indium doping is different, in order to make the indium doping completely, the different volumes of acetic acid are required. As a result, the 1 and 2 at.% indium doped ZnO need 0.1 and 0.18 acetic acids added in the initial solution to obtain low resistivity, respectively.

Figure 2 gives the XRD spectra of the single-layer ZnO:In thin films. From Fig. 2 it can be seen all the samples exhibit the typical hexagonal wurtzite structure. For the 1 at.% indium doped films, when the added acetic acid is below 0.1, the samples prefer to (002) orientation, and have strong (101) signal. However, for the acetic acid more than or equal to 0.1, the samples present (101) preferential orientation, the (100) and (002) orientations are strong. Besides, the (102) and (103) are also evident. The 2 at.% indium doped ZnO films have (101) prefer-orientation and strong (100) signal, the (002) signal is very weak. The intensities of the (002), (100) and (101) orientations of the film with 0.24 acetic acid are nearly the same.

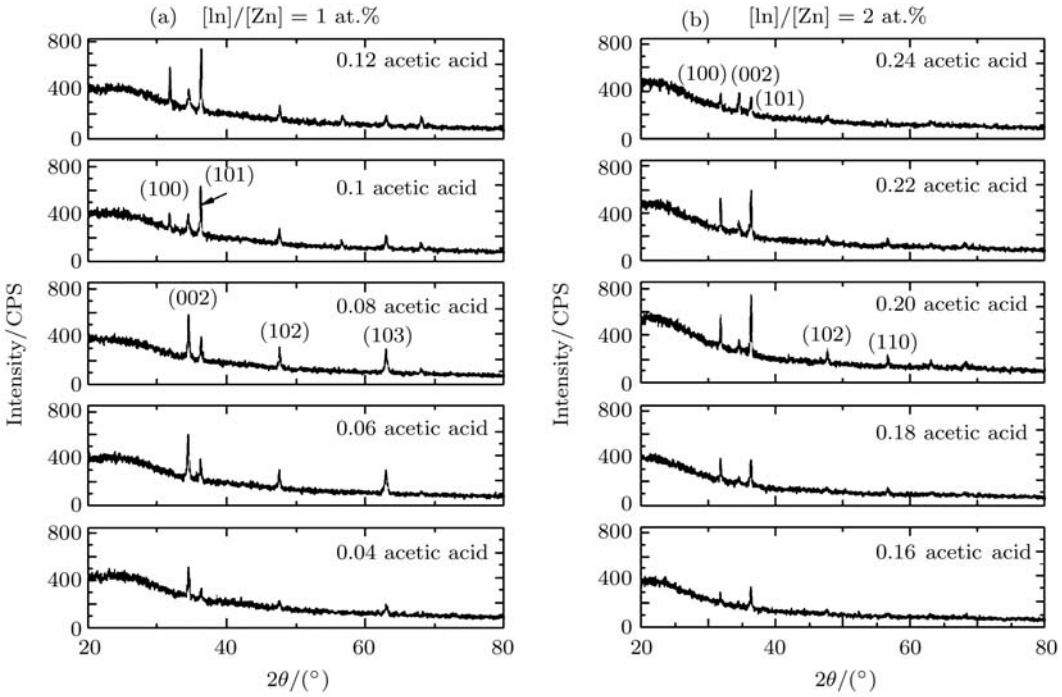


Fig. 2. XRD spectra of the single-layer ZnO:In films with different amounts of acetic acid added in the initial solution: (a) 1 at.% indium doped films, (b) 2 at.% indium doped films.

The surface morphology of the single-layer ZnO:In thin films can be observed by the SEM images shown in Fig. 3. For the 1 at.% indium doped thin films, when the acetic acid added is less than 0.1, the films exhibit hexagonal crystal growth and prefer to present triangle grains (see Figs. 3 (a)–3(c)). As the acetic acid added is more than or equal to 0.1, the films exhibit triangle grains with some cubic grains (see Figs. 3(d) and 3(e)). This is decided by the structure of the thin films. The schematic configuration of ZnO grains with the different growth orientations is given in Fig. 4. It can be seen that the surface morphologies of zinc oxide grains with (002) and (100) preferred orientations can form hexagonal and quadrilateral planes, respectively. The grain growing along with (101) orientation prefers to form the triangular pyramid. For the 1 at.% indium doped thin films, when the added acetic acid less than 0.1, the films prefer to grow hexagonal crystal due to (002) preferred orientation, and the grains with the preferential triangular pyramid shape are attributed to strong (101) signal. When the added acetic acid more than or equal to 0.1, the (101) prefer-orientation makes the films have triangle surface morphology. Moreover, there are some cubic grains due to the strong (100) and (002) orientations. This is in agreement with the results of XRD test. The triangle grains are in the pyramid-like shape. The pyramid-like surface is an effective light trapping structure, which is useful for the silicon thin-film solar cell.[19] For the 2 at.% indium doped films, all the samples have particle grains except the thin film with 0.24 acetic acid added (see Figs. 3(f)–3(j)), which is not suitable for the silicon thin-film solar cell. The films prefer (101) orientation and have strong (100) signal, the surface morphology trends to triangle and cubic grain. Moreover, the films have higher indium

doping (2 at.%), which can lower the structure properties of crystalline. Therefore, the small particle grains can be obtained. However, the 0.24 acetic acid added thin film exhibits columnar growth with small diameter, which are attributed to the growth orientation (see Fig. 2(b)) and higher indium doping.

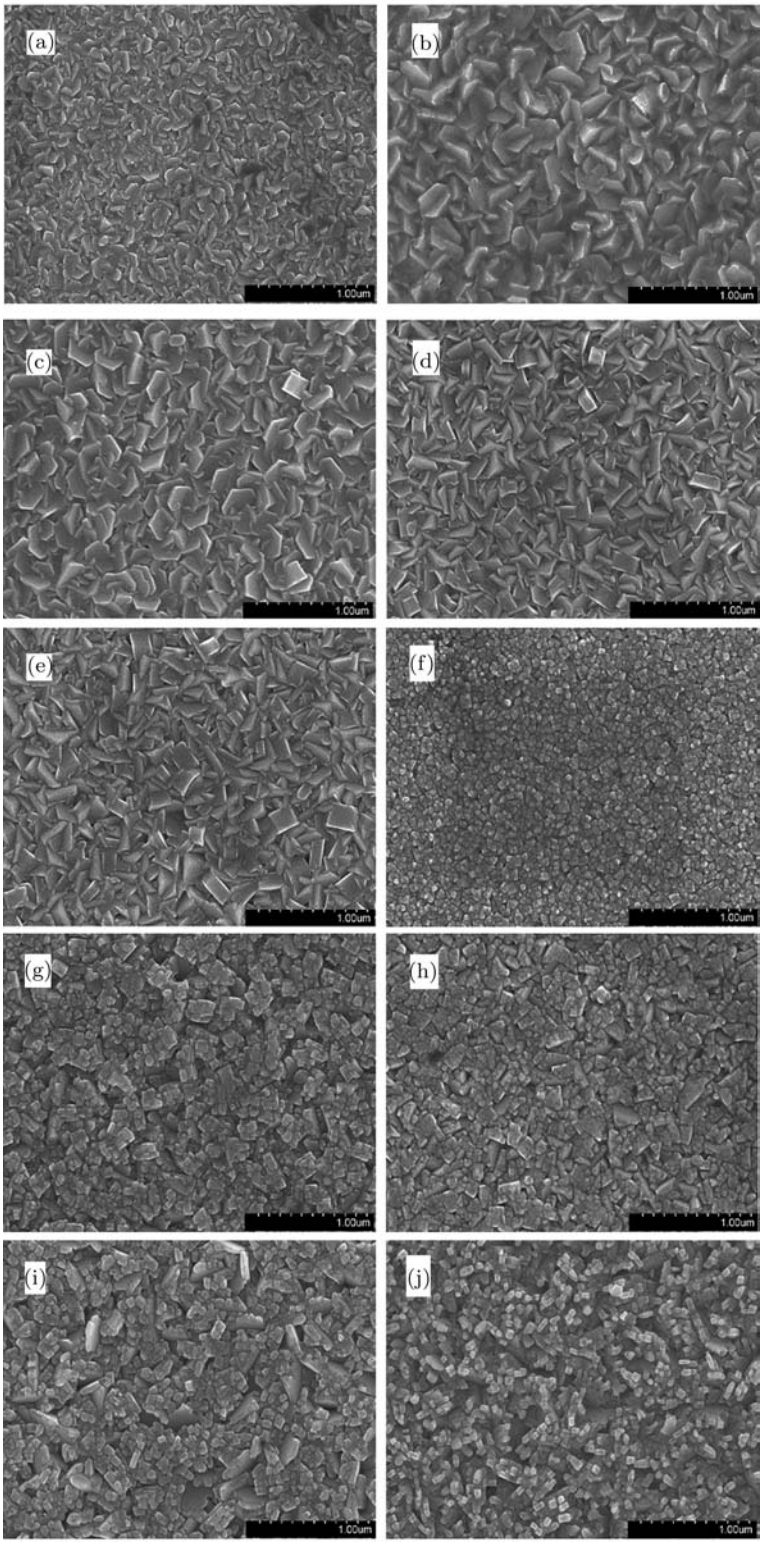


Fig. 3. (a)–(e). SEM images of the 1 at.% indium doped single-layer ZnO:In thin films with different amounts of acetic acid added in the initial solution ((a) 0.04, (b) 0.06, (c) 0.08, (d) 0.1, (e) 0.12). (f)∼(j). SEM images of the 2 at.% indium doped single-layer ZnO:In thin films with different amounts of acetic acid added ((f) 0.16, (g) 0.18, (h) 0.2, (i) 0.22, (j) 0.24).

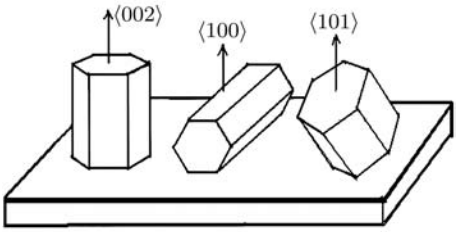


Fig. 4. Schematic configuration of ZnO grains with different growth orientations.

In conclusion, the 1 at.% indium doped single-layer ZnO film with 0.1 acetic acid added in the initial solution has good surface morphology of triangle pyramid-like shape. Its resistivity is 7.14×10^{-3} $\Omega\cdot$cm. For the 2 at.% indium doped, the lower resistivity (6.82×10^{-3} $\Omega\cdot$cm) can be achieved by the suitable acetic acid adding (0.18). But its morphology is particle.

3.2. Double-layer ZnO:In thin film property

It is well known that the substrate has a great effect on the film property. Based on the investigation of the single-layer ZnO:In thin films, in order to achieve good morphology and low resistivity at the same time, double-layer structure is designed. For convenience, the 1 at.% indium doped single-layer ZnO film with 0.1 acetic acid added in the initial solution is named as sample A, and the 2 at.% indium doped film with 0.18 acetic acid added is named as sample B. Samples A and B are used as substrate-layers, respectively. The following two group samples are prepared.

(1) Sample A is deposited as the substrate-layer. The 2 at.% indium doped ZnO thin films with different amounts of acetic acid are fabricated as the second-layers. Sample A has triangle surface morphology, and its resistivity is 7.14×10^{-3} $\Omega\cdot$cm.

(2) Sample B is used as the substrate-layer, and the second-layers are the 1 at.% indium doped films with different amounts of acetic acid added. Sample B has particle surface morphology, and its resistivity is 6.82×10^{-3} $\Omega\cdot$cm.

The electrical properties of the double-layer ZnO:In thin films are listed in Table 1. The resistivity of the double-layer films in group (1) does not change greatly. This trend is similar with the 2 at.% indium doped single-layers (see Fig. 1). The resistivity of the group (2) films decreases with increasing the acetic acid of the second-layer. It is the same as the 1 at.% indium doped single-layer (see Fig. 1). The 2 and 1 at.% indium doped single-layers are the second-layers of the group (1) and (2), respectively. Moreover, the substrate-layers of the two group films have almost the same resistivity. Hence, the resistivity of double-layer thin film varies with the second-layer. This leads to the natural conclusion that the resistivity of the second-layer has great effect on the double-layer ZnO:In thin film. When sample B as the second-layer is deposited on sample A, the lower resistivity (2.58×10^{-3} $\Omega\cdot$cm) can be achieved. Its mobility is 11.3 $\mathrm{cm^2\cdot V^{-1}\cdot s^{-1}}$, and its concentration is 2.14×10^{20} $\mathrm{cm^{-3}}$. Moreover, the low resistivity of single-layers (6.74×10^{-3} $\Omega\cdot$cm for 1 at.% indium doped with 0.1 acetic acid, 3.48×10^{-3} $\Omega\cdot$cm for 2 at.% indium doped with 0.18 acetic acid) can be obtained at the thicker thickness of 690 nm and 654 nm respectively, which are higher than the resistivity of double-layer.

Table 1. Electrical properties of the double-layer ZnO:In thin films.

group	substrate-layer	the second-layer	thickness/Å	sheet resistance /(Ω/□)	resistivity /Ω·cm	mobility /$\mathrm{cm^2\cdot V^{-1}\cdot s^{-1}}$	carrier concentration /$\mathrm{cm^{-3}}$
(1)	sample A	2 at.% in doped, 0.16 acetic acid	6359	65.81	4.19×10^{-3}	10.2	1.46×10^{20}
		2 at.% In doped, 0.18 acetic acid (sample B)	6396	40.34	2.58×10^{-3}	11.3	2.14×10^{20}
		2 at.% In doped, 0.20 acetic acid	6470	61.59	3.99×10^{-3}	12.2	1.28×10^{20}
		2 at.% In doped, 0.22 acetic acid	6433	90.36	5.81×10^{-3}	16.6	6.48×10^{19}

Table 1 *Continued*

group	substrate-layer	the second-layer	thickness/Å	sheet resistance /(Ω/□)	resistivity /Ω·cm	mobility /cm$^2\cdot$V$^{-1}\cdot$s^{-1}	carrier concentration /cm^{-3}
(2)	sample B	1 at.% in doped, 0.06 acetic acid	6192	299.26	1.85×10^{-2}	4.73	7.13×10^{19}
		1 at.% in doped, 0.08 acetic acid	6202	192.68	1.20×10^{-2}	4.03	1.30×10^{20}
		1 at.% in doped, 0.1 acetic acid (sample A)	6063	51.83	3.14×10^{-3}	8.50	2.34×10^{20}
		1 at.% in doped, 0.12 acetic acid	6461	50.46	3.26×10^{-3}	8.90	1.73×10^{20}

Figure 5 exhibits the XRD spectra of the double-layer ZnO:In thin films. All the double-layer ZnO:In thin films have (101) prefer-orientation and strong (100) signal. The structure characteristics of both the substrate-layer and the second-layer can be explicated in the XRD spectrum of the double-layer thin film. The diffraction peak of the substrate-layer can emerge in the spectrum of double-layer film. Both sample A and B prefer (101) and have strong (100) signal (see Fig. 2.), which are used as substrate-layers for group (1) and (2) films respectively. Hence, the double-layer films all exhibit (101) preferentially orientation and strong (100) peak.

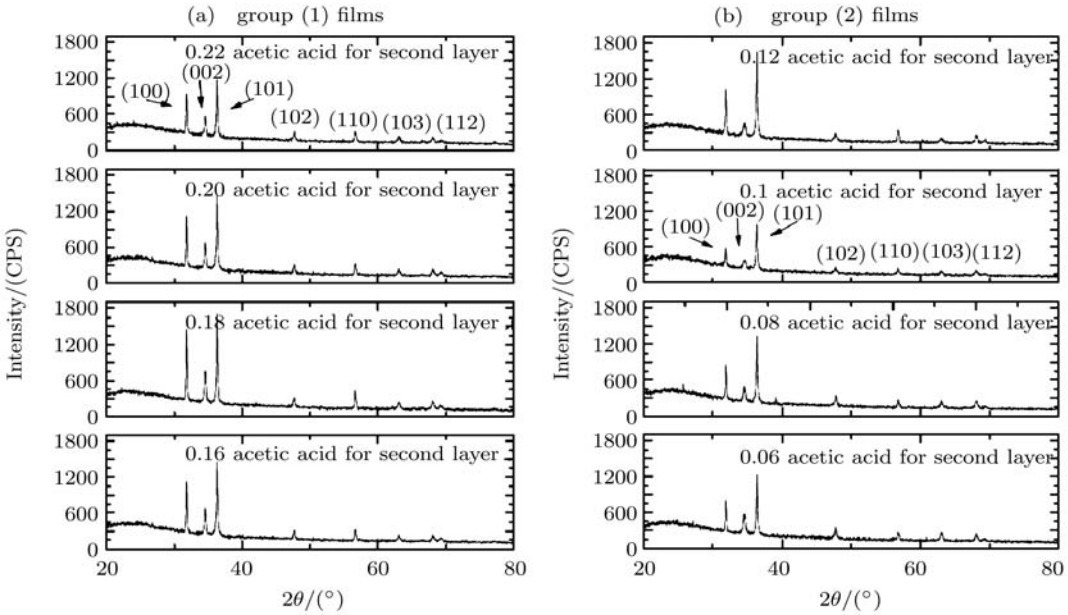


Fig. 5. XRD spectra of the double-layer ZnO:In thin films. (a) Group (1) films: sample A as the substrate-layer, the 2 at.% indium doped single-layer films with different acetic acid added as the second-layers. (b) Group (2) films: sample B as the substrate-layer; the 1 at.% indium doped single-layer films with different acetic acid added as the second-layers.

The SEM images of the double-layer ZnO:In thin films and the ASAHI U-type SnO_2:F are given in Fig. 6. Through the above discussion, the similar structure properties can lead to the similar surface morphologies. Although the double-layer ZnO:In films have similar XRD spectra, the SEM images are different. The group (1) double-layer films have triangle grains (See Figs. 6(a)–(d)). Sample A with triangle grains is used as the substrate-layer. The second-layer with particle morphology can grow along with the triangle grain. Therefore, the group (1) double-layer films have triangle morphology. For the group (2) double-layer films, most of the grains have particle shape. In addition, a few of triangle grains is not evident (See Figs. 5(e)–(h)). When the second-layer with triangle grains is prepared on the substrate-layer with particle surface, the second-layer can grow along with the particle grain. However, the second-layer

has the trend to form triangle. Therefore, the particle and triangle morphologies can be obtained at the same time. In conclusion, the surface morphology of double-layer ZnO:In thin films is mainly decided by the substrate even though the second-layer also affect the surface morphology of double-layer film. The double-layer film obtained by depositing sample B on sample A has triangle grains, in pyramid-like shape, which is suitable for the silicon thin-film solar cell (see Fig. 5(b)).

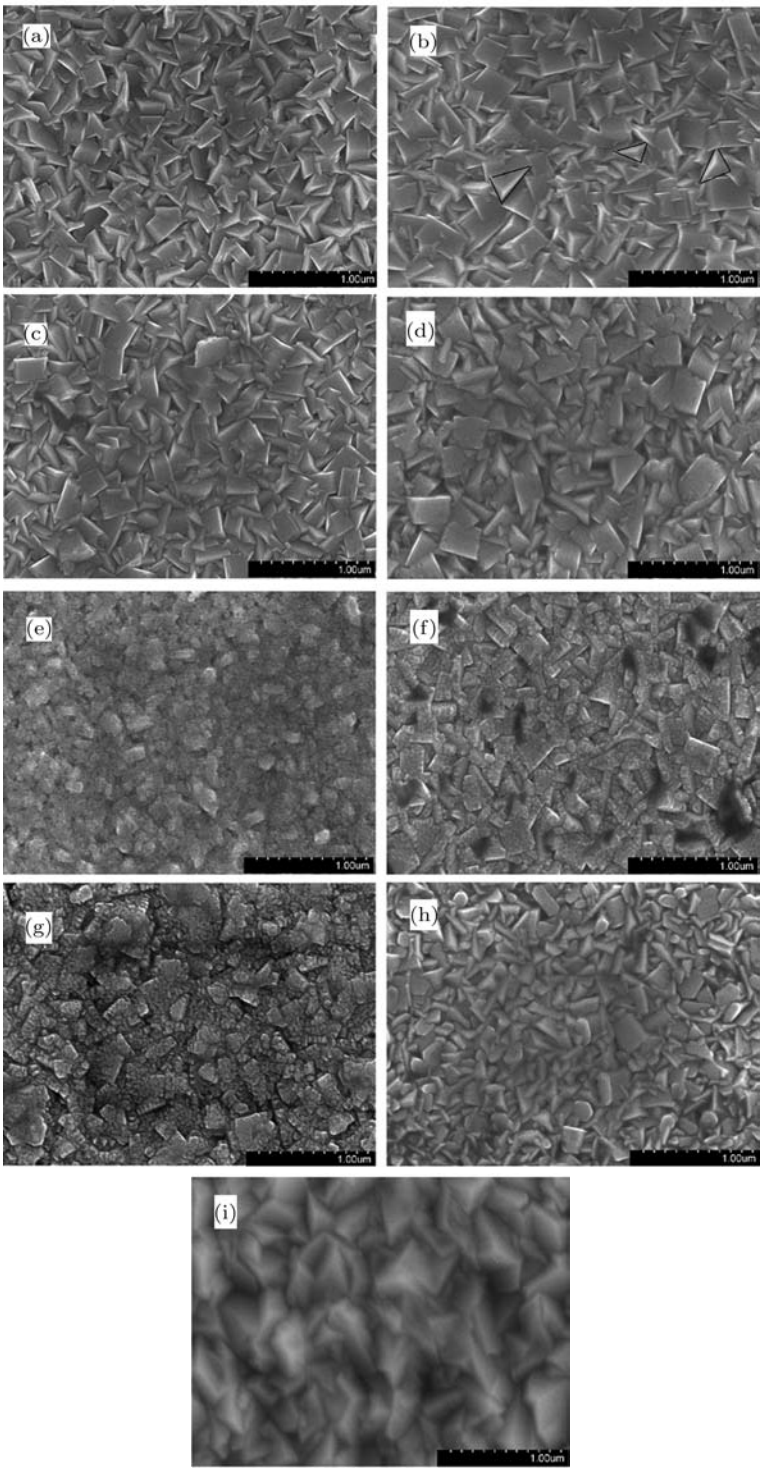


Fig. 6. SEM images of the double-layer ZnO:In films. (a)–(d). Group (1) films: sample A as the substrate-layer and the 2 at.% indium doped single layer as second-layer with different amounts of acetic acid added in the initial solution ((a) 0.16, (b) 0.18, (c) 0.2, (d) 0.22). (e)–(h). Group (2) films: sample B as the substrate-layer and the 1 at.% indium doped single layer as second-layer with different amounts of acetic acid added ((e) 0.06, (f) 0.08, (g) 0.1, (h) 0.12). (i). SEM image of ASAHI U-type SnO_2:F.

3.3. Solar cell performance

Among the double-layer ZnO:In films, the film obtained by depositing sample B on the sample A not only has the lowest resistivity (2.58×10^{-3} $\Omega\cdot$cm), but also has good surface morphology of triangle pyramid-like shape. It is suitable for the silicon thin-film solar cells as TCO. This double-layer ZnO:In thin film and the ASAHI U-type SnO_2:F are used as front electrodes in single junction a-Si:H solar cells. Table 2 gives some properties of the two TCO films including the electrical and optical properties. The δ_{rms} obtained by AFM is also listed. Although the thickness of the double-layer ZnO:In thin film (6396 Å) is smaller than the SnO_2:F (9000 Å), the δ_{rms} of the two TCOs is approximately the same (35.11 nm for double-layer ZnO:In, 30.27 nm for SnO_2:F). The sheet resistance of the double-layer ZnO:In (40.34 $\Omega/\square$) is larger than SnO_2:F (8.56 $\Omega/\square$). However, the total transmittance of the double-layer ZnO:In is higher than the SnO_2:F. More details are given in Fig. 7. The total and direct transmittance and the haze factor of the two TCOs are shown in Fig. 7. The haze factor is defined as (total transmittance - direct transmittance)/total transmittance $\times$ 100%. It can be seen that the total and direct transmittances of the double-layer ZnO:In are higher than SnO_2:F. However the haze factor of the double-layer ZnO:In is lower than the SnO_2:F. The SEM images of the two TCOs are given in Figs. 6(b) and 6(i), respectively. The double-layer ZnO:In has triangle pyramid-like shape, and the SnO_2:F has typical pyramid-like surface morphology.

Table 2. Properties of the sprayed double-layer ZnO:In thin film and the ASAHI U-type SnO_2:F.

TCO	thickness/Å	sheet resistance /($\Omega/\square$)	resistivity /$\Omega\cdot$cm	average total transmittance /(400–800 nm)	δ_{rms} (AFM) /nm
ZnO:In double-layer by USP	6396	40.34	2.58×10^{-3}	84.30%	35.11
ASAHI U-type SnO_2:F	9000	8.56	7.71×10^{-4}	79.14%	30.27

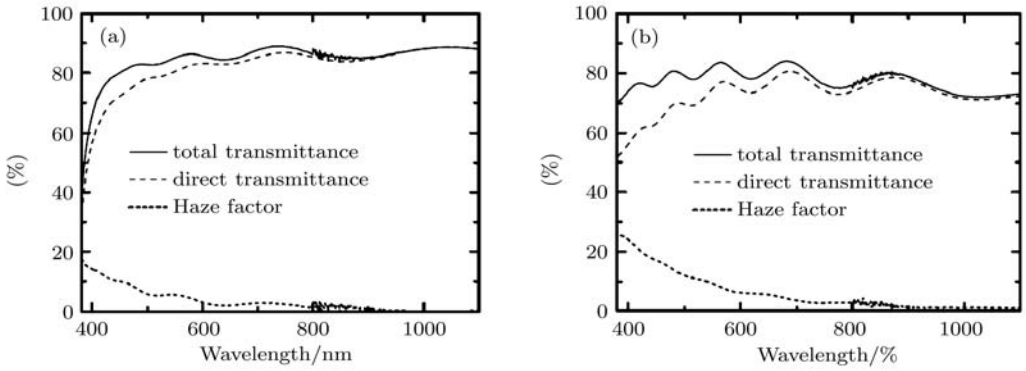


Fig. 7. Optical properties of the double-layer ZnO:In thin film by USP (a) and the ASAHI U-type SnO_2:F (b). Solid, dash and dot stand for total transmittance, direct transmittance and haze factor, respectively.

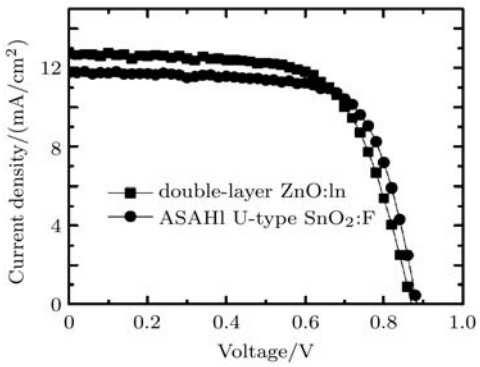


Fig. 8. Light J–V curves of single junction a-Si:H solar cells on the double-layer ZnO:In thin film by USP (square) and the ASAHI U-type SnO_2:F (circle) as front electrodes.

Single junction a-Si:H solar cells were fabricated on both the double-layer ZnO:In and the ASAHI U-type SnO_2:F. The measured J–V characteristics of both the solar cells are presented in Fig. 8, and the corresponding parameters are listed in Table 3. The open circuit voltage (V_{oc}) and conversion efficiency (η) of the cell deposited on the SnO_2:F is slightly higher (V_{oc} 0.88 V, η 7.31%) than the double layer ZnO:In film (V_{oc} 0.87 V, η 7.26%). The obvious differences of the cells on the two TCOs exist both in the short circuit current density J_{sc} and the fill factor (FF). The J_{sc} of single junction a-Si:H solar cell on the double-layer ZnO:In (12.696 mA/cm^2) is higher

than the SnO_2:F (11.775 mA/cm^2), which is mainly caused by the higher transmittance of the double layer ZnO:In. However the FF of solar cells on the double-layer ZnO:In (0.66) is lower than the the SnO_2:F (0.7), which is mainly caused by the higher resistivity of the double-layer ZnO:In.

Table 3. Comparison of the performance of single junction a-Si:H solar cells on the double-layer ZnO:In thin film and the ASAHI U-type SnO_2:F as front electrodes.

front electrode	η/%	V_{oc}/V	J_{sc}/(mA/cm^2)	FF
ZnO:In double-layer by USP	7.26	0.87	12.70	0.66
ASAHI U-type SnO_2:F	7.31	0.88	11.78	0.70

4. Conclusions

The ZnO:In thin films were prepared by a low-cost USP. The 1at.% indium doped single-layer ZnO:In thin film with 0.1 acetic acid added in the initial solution showed good triangle surface morphology, which is very useful for the silicon thin-film solar cell. Through the investigation on the double-layer ZnO:In thin films, it is found that the surface morphology is mainly decided by the substrate-layer; and the second-layer has great effect on the resistivity of the double-layer ZnO:In thin film. The 2 at.% indium doped single-layer ZnO thin film with 0.18 acetic acid had lower resistivity (6.82×10^{-3} $\Omega\cdot$cm). It was deposited on the single-layer ZnO film with 1 at.% indium doped and 0.1 acetic acid added, which had triangle grains. Through this method, the double-layer ZnO:In with good electrical properties (2.58×10^{-3} $\Omega\cdot$cm) and triangle surface morphology was obtained. The double-layer ZnO:In film was compared to the ASAHI U-type SnO_2:F. The Sheet resistance of the double-layer ZnO:In (40.34 $\Omega/\Box$) is higher than the SnO_2:F (8.56 $\Omega/\Box$). Both the total and direct transmittances of the double-layer ZnO:In are above 80% in the visible range, which is higher than the SnO_2:F. Both the two TCOs are used as front electrodes in single junction a-Si:H solar cells. The J_{sc} of the solar cell on the double-layer ZnO:In is higher than SnO_2:F. This leads to the nature conclusion that the sprayed ZnO:In films with good properties can be obtained by the double-layer structure.

References

[1] Look D C 2001 *Mater. Sci. Eng.* B **80** 383

[2] Han X Y, Hou G F, Wei C C, Zhang X D, Dai Z H, Li G J, Sun J, Chen X L, Zhang D K, Xue J M, Zhao Y and Gen X H 2009 *Acta Phys. Sin.* **58** 4254 (in Chinese)

[3] Zhang X D, Zhao Y, Sun F H, Wang S F, Han X Y, Wei C C, Sun J, Geng X H and Xiong S Z 2009 *Acta Phys. Sin.* **58** 5041 (in Chinese)

[4] Zhang X D, Zhao Y, Gao Y T, Chen F, Zhu F, Wei C C, Sun J, Geng X H and Xiong S Z 2006 *Acta Phys. Sin.* **55** 6697 (in Chinese)

[5] Fay S, Steinhauser J, Nicolay S and Ballif C 2010 *Thin Solid Films* **518** 2961

[6] Fay S, Feitknecht L, Schluchter R, Kroll U, Vallat-Sauvain E and Shah A 2006 *Sol. Energy Mater. Sol. Cells* **90** 2960

[7] Chen X L, Geng X H, Xue J M, Zhang D K, Hou G F and Zhao Y 2006 *J. Cryst. Growth* **296** 43

[8] Chen X L, Xu B H, Xue J M, Zhao Y, Wei C C, Sun J, Wang Y, Zhang X D and Geng X H 2007 *Thin Solid Films* **515** 3753

[9] Anna Selvana J A, Delahoy A E, Guo S and Li Y M 2006 *Sol. Energy Mater. Sol. Cells* **90** 3371

[10] Duenow J N, Gessert T A, Wood D M, Young D L and Coutts T J 2008 *J. Non-Cryst Solids* **354** 2787

[11] Lucio-Lopez M A, Luna-Arias M A, Maldonado A, Olvera M de la L and Acosta D R 2006 *Sol. Energy Mater. Sol. Cells* **90** 733

[12] Lee C, Lim K and Song J 1996 *Sol. Energy Mater. Sol. Cells* **43** 37

[13] Benouis C E, Benhaliliba M, Juarez A S, Aida M S, Chami F and Yakuphanoglu F 2010 *J. Alloy Compd.* **490** 62

[14] Wienke J and Booij A S 2008 *Thin Solid Films* **516** 4508

[15] Wienke J, van der Zanden B, Tijssen M and Zeman M 2008 *Sol. Energy Mater. Sol. Cells* **92** 884

[16] Olvera M de la L, Maldonado A, Asomoza R and Melendez-Lira M 2002 *Sol. Energy Mater. Sol. Cells* **71** 61

[17] Maldonado A, Asomoza R, Canetas-Ortega J, Zironi E P Hernandez R, Patino R and Solorza-Feria O 1999 *Sol. Energy Mater. Sol. Cells* **57** 331

[18] Analytical Chemistry staff room of Hangzhou University 1997 *Handbook of Analytical Chemistry (*the first volumes: *Basic and Safety knowledge)* (2nd ed) (Beijing: Chemical Industry Press) p160 (in Chinese)

[19] Müller J, Rech B, Springer J and Vanecek M 2004 *Sol. Energy* **77** 917